Anion Vacancy Distribution and Magnetism in the New Reduced Layered Co(II)/Co(I) Phase $LaSrCoO_{3.5-x}$

M. A. Hayward and M. J. Rosseinsky*

Department of Chemistry, University of Liverpool, Crown Street, Liverpool, L69 7ZD, United Kingdom

Received October 26, 1999. Revised Manuscript Received May 2, 2000

The new reduced K_2NiF_4 Co(II) phase, $LaSrCoO_{3.5-x}$, is prepared by reduction of the Co(III) containing $LaSrCoO_4$ using H_2 gas and the new hydride solid−solid reduction methods. The hydride route is superior in both crystallinity and control of phase purity and allows access to reduced phases containing substantial concentrations of Co(I). The anion vacancies are located within the MO_2 planes of the K_2NiF_4 structure but do not prevent the onset of long-range antiferromagnetic order: the magnetic structure is refined using a noncollinear model consistent with the tetragonal crystal symmetry.

Introduction

A wide variety of vacancy-ordered derivatives of reduced perovskites are now known, with the precise ordering pattern being determined by the electronic structure (oxidation and spin state) of the transition metal ion: $La_2Ni_2O_5$ features d^8 Ni(II) in both octahedral and square planar environments,[1] the common brownmillerite structure of $Ca_2Fe_2O_5$ contains alternating layers of octahedral and tetrahedral metal centers,[2] $CaMnO_{2.5}$ and $Ca_2MnO_{3.5}$ contain manganese in five-coordinate square pyramidal environments,[3,4] $(La,Sr)_8Cu_8O_{20}$ has copper cations in 4-, 5-, and 6-fold coordination.[5]

Recent work on the reduction of $LaCoO_3$ revealed $La_3Co_3O_8$ (an octahedral/tetrahedral phase) as an intermediate on the pathway to the brownmillerite $La_2Co_2O_5$.[6,7] This phase, which contains high-spin Co(II) consistent with the 9.8% volume expansion on reduction from low-spin Co(III) in $LaCoO_3$, orders antiferromagnetically in a G-type structure below 310 K, with moments at both octahedral and tetrahedral sites consistent with the spin-state assignment.

The above reports of reduction of three-dimensional perovskite phases involve synthesis at relatively high temperatures, typically by Zr gettering at 400 °C. In this paper we report the reduction of the two-dimensional K_2NiF_4 phase $LaSrCoO_4$ using both H_2 gas and the newly introduced low-temperature agent for topotactic oxide deintercalation, NaH. This reagent is able to effect reduction reactions at considerably lower temperatures than conventional techniques and has allowed the isolation of $LaNiO_2$,[8] resolving an outstanding issue concerning this phase, which has long been difficult to synthesize. The new reagent is found to be superior in terms of crystal quality and stoichiometry control; cobalt mean oxidation states below Co(II) are accessible when the NaH reduction technique is employed, indicating that further reduction is possible than for the perovskite. The vacancies thus formed are located in the transition metal BO_2 layers but are not ordered on a neutron/X-ray diffraction length scale: the reduction produces a disordered rotation of the metal coordination polyhedra. The reduced phases are magnetically ordered with $T_N \approx 110$ K and a noncollinear magnetic structure consistent with the tetragonal symmetry is deduced.

Experimental Section

Synthesis. *Starting Materials.* Five-gram samples of $LaSrCoO_4$ were synthesized via a citrate precursor method. Stoichiometric amounts of La_2O_3 (Aldrich, 99.999%, which had been previously dried at 1000 °C in air), $SrCO_3$ (Alfa, 99.994%), and cobalt powder (Alfa, 99.985%) were dissolved in a minimum quantity (typically 150 mL) of a 1:1 solution of 6 M nitric acid and distilled water. Five milliliters of analar ethylene glycol (Aldrich, >99%) and 6.734 g (3.5×10^{-2} moles) of citric acid (Fischer, >99.5%) were subsequently added and the solution was heated at 150 °C, with constant stirring, for approximately 3 h. The gel thus formed was decomposed by further heating at 300 °C and then 600 °C, in air, for 24-h periods to complete the decomposition of the organic components of the mixture. The resulting black powder was then pressed into 13-mm diameter pellets at 5 ton of pressure and annealed at 1300 °C for 2 periods of 36 h, under flowing oxygen, with regrinding between heating periods. Powder X-ray diffraction data were found to be in good agreement with published data for $LaSrCoO_4$ ($a = 3.8075(2)$ Å, $c = 12.4984(7)$ Å. Published data: $a = 3.806$ Å, $c = 12.500$ Å[9]). Thermogravimetric analysis (via complete hydrogen reduction to La_2O_3, SrO, and cobalt metal with product identity confirmed by subsequent powder X-ray diffraction) of the cobalt oxidation state indicated, within error, no significant deviation from the

(1) Alonso, J. A.; Martinez-Lope, M. J. *J. Chem. Soc., Dalton Trans.* **1995**, *17*, 2819.
(2) Berggren, J. *Acta Chem. Scand.* **1971**, *25*, 3616.
(3) Leonowicz, M. E.; Poeppelmeier, K. R.; Longo, J. M. *J. Solid State Chem.* **1985**, *59*, 71.
(4) Poeppelmeier, K. R.; Leonowicz, M. E.; Longo, J. M. *J. Solid State Chem.* **1982**, *45*, 71.
(5) Errakho, L.; Michel, C.; Raveau, B. *J. Solid State Chem.* **1988**, *73*, 514.
(6) Hansteen, O. H.; Fjellvag, H.; Hauback, B. C. *J. Mater. Chem.* **1998**, *8*, 2081.
(7) Hansteen, O. H.; Fjellvag, H.; Hauback, B. C. *J. Solid State Chem.* **1998**, *141*, 411.
(8) Hayward, M. A.; Green, M. A.; Rosseinsky, M. J.; Sloan, J. *J. Am. Chem. Soc.* **1999**, *121*, 8843.
(9) Demazeau, G.; Courbin, P.; Le Flem, G.; Pouchard, M.; Hagenmuller, P.; Soubeyroux, J. L.; Main, I. G.; Robins, G. A. *Nouv. J. Chim.* **1979**, *3*, 171.

10.1021/cm9906811 CCC: $19.00
Published on Web 07/06/2000

ideal stoichiometry of $LaSrCoO_4$ in all samples (calculated stoichiometry: $LaSrCoO_{4.00(1)}$)

Reduction of $LaSrCoO_4$. The reduction of $LaSrCoO_4$ was performed via two synthetic routes. The first (sample A) involved heating a finely ground 5-g sample of $LaSrCoO_4$ contained within an alumina crucible under a flow of 8% H_2 in N_2 (Air Products, dried by passing through a column containing 4-Å molecular sieves (BDH)) within a silica flow tube, at a temperature of 550 °C for 4 h. The second method involved direct reaction with sodium hydride (NaH) in a manner similar to that described in the study of $LaNiO_2$.[8] Typically, 5 g (1.43×10^{-2} mol) of $LaSrCoO_4$ was ground with a double stoichiometric excess (686 mg, 2.86×10^{-2} mol) of NaH in a He-filled Mbraun Labmaster drybox and then sealed in an evacuated Pyrex ampule ($p < 2 \times 10^{-4}$ Torr). The sealed reaction vessel was then treated in one of two heating regimes: sample B was heated for 2 periods of 5 days, at 200 °C, with intermediate regrinding; sample C was heated for 3 periods of 4 days, at 200 °C, with intermediate regrinding. The reaction products were then washed with CH_3OH to remove the NaOH (produced as a reaction byproduct) and any unreacted NaH from the reaction mixture. Typically, 5×60 mL of CH_3OH (which had been previously dried by distillation from Mg) was transferred via cannula onto the reaction products in a 100-mL filter Schlenk, under a nitrogen atmosphere. The suspension was then vigorously agitated, for 1 min, to allow the sodium-containing phases to react with, and dissolve in, the solvent, before being filtered. The washed reaction products were then dried under vacuum ($p < 10^{-1}$ Torr). Energy-dispersive X-ray (EDX) analysis was performed on a large number of crystallites, using a JEM-2010 microscope fitted with a windowless Si(Li) detector and operated using the LINK "pentafet" EDX microanalysis system, to ensure no residual sodium remained in the samples. Close inspection of powder X-ray diffraction patterns collected from samples before and after the washing procedure indicate that the lattice parameters of the reduced cobaltate phase do not change, within error ($a = 3.745(1)$ Å, $c = 13.260(3)$ Å unwashed; $a = 3.7454(9)$ Å, $c = 13.263(3)$ Å after being washed), and that the full-width at half-maximum (fwhm) of diffraction reflections are actually slightly smaller after washing.

Annealing experiments were performed on $LaSrCoO_{3.5-x}$ samples which were loaded, in a He-filled glovebox, into thoroughly dried Pyrex ampules and sealed with a torch, under vacuum ($p < 10^{-4}$ Torr). In addition, some samples were sealed in ampules with Zr or Li getters, such that the $LaSrCoO_{3.5-x}$ was not in physical contact with the getter, but shared the same atmosphere within the sealed evacuated Pyrex apparatus.

Structural Characterization. Neutron powder diffraction data were collected at 298 K from 5-g samples (which were indium-sealed in vanadium cans under helium) utilizing the backscattering ($160 \leq 2\theta/° \leq 176$) and 90° ($87 \leq 2\theta/° \leq 93$) detector banks on the HRPD instrument at the ISIS spallation neutron source, Rutherford Appleton Laboratory, United Kingdom. Diffraction data were also collected on samples sealed in vanadium cans under argon on the D2B diffractometer at the Institut Laue Langevin, Grenoble, at 5 K using a wavelength of 1.59 Å and at wavelengths of 1.59 and 2.38 Å (with a pyrolytic graphite filter to suppress higher harmonics of the fundamental wavelength) at 298 K.

X-ray powder diffraction data were collected from samples loaded, within a helium-filled glovebox, into a sealed sample stage using a Siemens D5000 diffractometer in Bragg–Brentano geometry employing Cu $K\alpha_1$ radiation from a quartz monochromator.

Rietveld profile refinement was performed on the powder diffraction data using the GSAS suite of programs[10] employing a pseudo-Voigt peak shape in the case of constant wavelength data and a convolution of pseudo-Voigt and Ikeda-Carpenter functions in the case of time-of-flight data. Refinements employed a 16-term cosine Fourier series background function.

Thermogravimetric measurements were performed using a Rheometric Scientific STA 1500 thermal analyzer. Measurements to analyze the reduction behavior of $LaSrCoO_4$ were performed on samples of around 50 mg which were loaded into platinum crucibles and then heated at 4 °C min^{-1} under flowing, dried 8% H_2 in N_2 (Air Products). Reoxidation measurements to calculate the oxidation states of reduced materials were performed on 50-mg samples which were rapidly loaded into platinum crucibles and then heated at 4 °C min^{-1} under flowing oxygen (Air Products). The identity and oxygen stoichiometry of the reoxidized products were determined by X-ray powder diffraction and immediate complete thermogravimetric reduction after the reoxidation, respectively.

Magnetic data were collected, on samples contained within sealed gelatine capsules (which had been previously loaded in the drybox), using a Quantum Design MPMS SQUID magnetometer.

All samples were found to be contaminated by very small (maximum observed amount, ~1.4 mol %; minimum, ~0.3 mol %; calculated from magnetization measurements) quantities of a ferromagnetic impurity assigned as cobalt metal. It is assumed that this impurity is formed by the reduction of very small quantities of binary cobalt oxides remaining from the incomplete synthesis of the $LaSrCoO_4$ starting material as the quantity of impurity observed appears to be directly related to the particular batch of starting material which is reduced rather than the reduction method employed. It should be noted that no Bragg reflections could be assigned as cobalt metal in any of the diffraction patterns collected.

The paramagnetic susceptibility of the bulk $LaSrCoO_{3.5-x}$ material was measured by saturating the ferromagnetic part of the signal (in fields larger than 2 T) and then measuring magnetization–field isotherms. The paramagnetic susceptibility of the sample was taken to be the slope of the linear high-field sections of these plots. To this end a sample of $LaSrCoO_{3.38}$ (23 mg) prepared via the NaH reduction method (sample C) was cooled in a 2-T field to 5 K. The magnetization of the sample was then measured in 11 fields from 2 to 3 T (1000-G steps) to measure the paramagnetic susceptibility of the sample accurately. This procedure was then repeated at 5 K temperature intervals from 5 to 300 K. The magnetization–field isotherms were fitted to a linear function, with data points with large errors being excluded from the fit. All fits had at least nine points.

Results

Thermogravimetric analysis of the reduction of $LaSrCoO_4$ with 8% H_2 in N_2 indicates the presence of a stable phase of composition $LaSrCoO_{3.496(3)}$ as shown in Figure 1. Repeating the reduction on a larger scale at 550 °C yielded a phase which could be readily indexed in the $I4/mmm$ space group with lattice parameters $a = 3.745$ Å, $c = 13.286$ Å, and $V = 186.33$ Å^3.

Rietveld profile refinement of time-of-flight neutron powder diffraction data collected on the HRPD instrument and laboratory X-ray powder diffraction data from a 5-g sample prepared by the hydrogen reduction of $LaSrCoO_4$ (sample A) was performed employing a model based on the K_2NiF_4 structure of $LaSrCoO_4$[9] with refined oxide ion occupancies. Close inspection of the neutron powder diffraction data revealed Bragg reflections due to a small amount (~0.8 mol %) of $LaSrCoO_4$ starting material which was inserted as a second phase in the refinement. The fit to the data employing one reduced phase is rather poor ($\chi^2 = 4.7$) as shown in Figure S1 (Supporting Information). A large number of the Bragg reflections are fitted well but a significant number, especially at large times-of-flight, have signifi-

(10) Larson, A. C.; Von Dreele, R. B. *General Structural Analysis System*; Los Alamos National Laboratory: Los Alamos, NM, 1994.

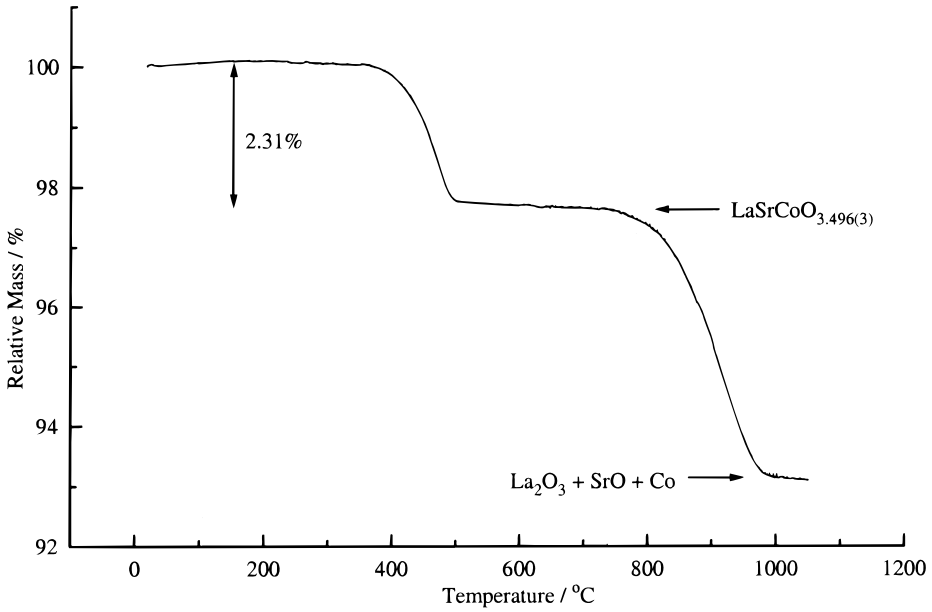

Figure 1. Thermogravimetric data for the reduction of $LaSrCoO_4$ with 8% H_2 in N_2. A mass loss of 2.28% is expected for the formation of the pure Co(II) phase $LaSrCoO_{3.5}$.

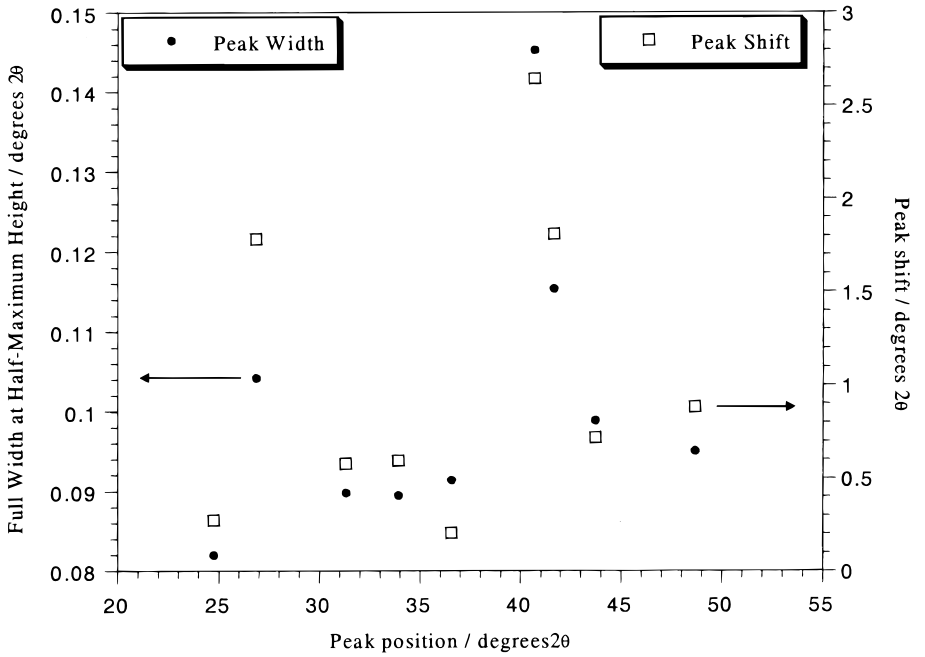

Figure 2. Full-width at half-maximum height (fwhm) of X-ray powder diffraction reflections of $LaSrCoO_{3.51(3)}$ synthesized by hydrogen reduction plotted with the measured peak shift upon reduction against peak position in 2θ.

cant errors. Measuring the fwhm of diffraction reflections in an X-ray diffraction pattern of this material revealed a number of especially broad reflections. However, there was no systematic relation between these broad reflections to indicate a lowering of cell symmetry or any obvious anisotropic broadening axis. Plotting the fwhm of reflections along with the peak shift observed, in 2θ, of each reflection in the transformation from $LaSrCoO_4$ to $LaSrCoO_{3.5-x}$ against the position of each peak in 2θ demonstrates that there is a direct correlation between the peaks which are shifted a large distance upon reduction and peaks with large fwhm's as shown in Figure 2. This observation would suggest that the sample contains a range of local oxygen stoichiometries, each with an appropriate set of lattice parameters (ranging from that of the least reduced region to those of the most reduced region of the sample), and that the data would be best modeled using a multiphase description.

To this end a second $LaSrCoO_{3.5-x}$ phase was added to the refinement model, with the thermal parameters of the metal ions and the Gaussian profile parameters of the two phases constrained to be the same. The fit to the experimental data was significantly improved by the introduction of a two-phase model ($\chi^2 = 2.5$).

There were however problems with the highly anisotropic displacement parameter for the oxygen anions within the MO_2 transition metal layers at the position ($^1/_2$, y, 0) in both phases (the size of the displacement parameter refined to be 15 times greater parallel to the x axis than to the y axis). The most physically reasonable way to model the scattering around this position

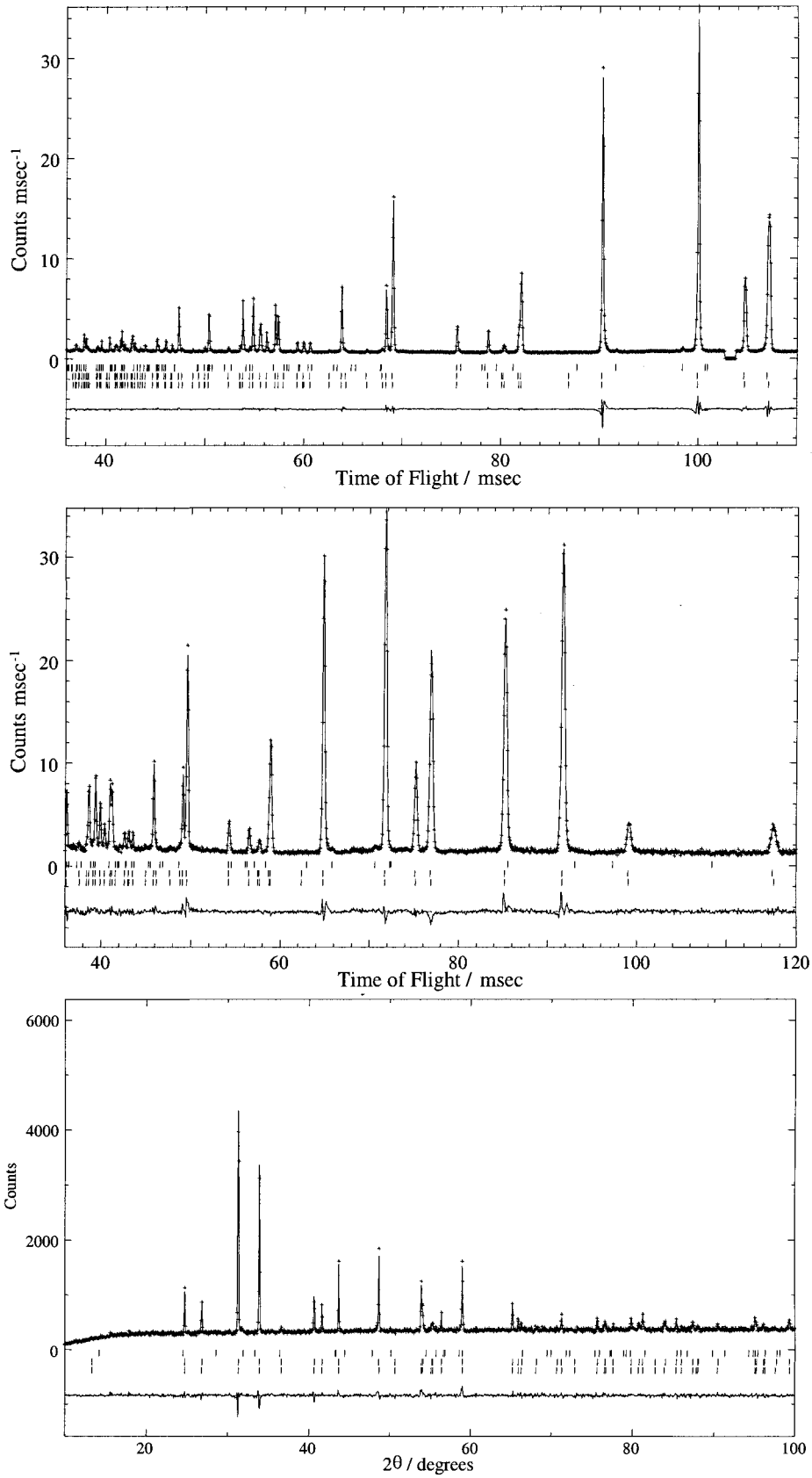

Figure 3. Observed, calculated, and difference plots for the Rietveld profile refinement of a (a) HRPD backscattering bank, (b) HRPD 90° bank, and (c) powder X-ray diffraction data collected from a 5-g sample of $LaSrCoO_{3.51(3)}$ reduced under flowing 8% H_2/N_2 employing a model with two $LaSrCoO_{3.5-x}$ phases (bottom tick marks, phase 1; middle tick marks, phase 2) and a $LaSrCoO_4$ phase (upper tick marks).

was to insert an additional oxide ion at a ($^1/_2$, y', 0) site and then refine the positions of these two oxide ions independently.

The results of the refinement employing two reduced $LaSrCoO_{3.5-x}$ phases are shown in Figure 3; Figure 4 shows the refined disordered structure, with structural

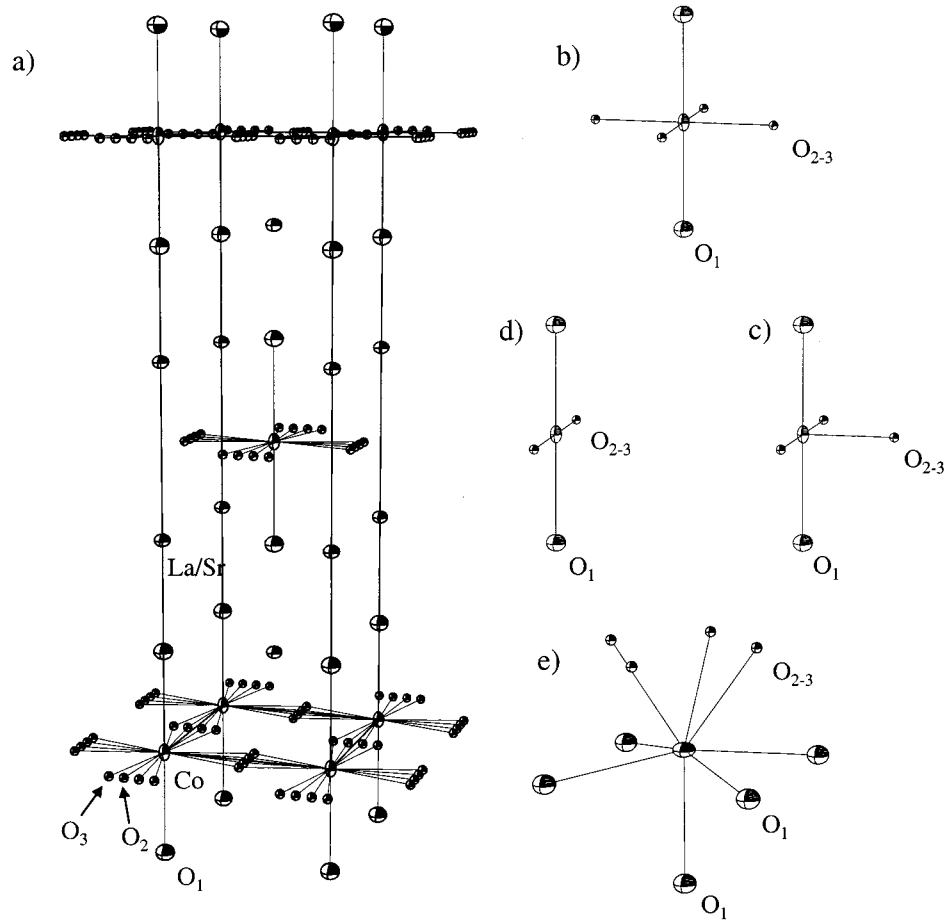

Figure 4. (a) The refined structure of $LaSrCoO_{3.432(8)}$ illustrating the disordered oxide ion vacancies in the CoO_{2-x} planes (O_2 fraction: 0.179(1); O_3 fraction: 0.179(1)) and their effects on the possible local coordination polyhedra which can be constructed around cobalt: (b) a six-coordinate elongated octahedron, (c) a five-coordinate distorted rectangle-based pyramid, (d) a four-coordinate rectangular planar configuration, and (e) the local coordination around the lanthanum/strontium position. The partial occupancy of the O_{2-3} anions lowers the mean La/Sr coordination number to 7.86(2).

data in Table 1 and refined bond lengths in Table 3. The key difference between the two refined phases is the number of oxide ion vacancies exhibited by each and the associated level of distortion of their resulting structures away from that of $LaSrCoO_4$. The two refined phases show that reduction of $LaSrCoO_4$ to $LaSrCoO_{3.5-x}$ occurs via the topotactic deintercalation of oxide ions from the ($^1/_2$, 0, 0) position within the CoO_2 layers in the (La/Sr)O−(La/Sr)O−CoO_2−(La/Sr)O−(La/Sr)O stacking sequence to form a layer of stoichiometry $CoO_{2-(0.5+x)}$ ($x = 0.068$, phase 1; $x = -0.076$, phase 2). The cobalt−oxygen coordination polyhedra, which can be constructed from the refined structure, are highly unusual. The refined stoichiometries of the two reduced phases suggest the existence of 4-, 5-, and 6-fold coordinate cobalt. Of the possible coordination polyhedra which can be constructed, within the limits imposed by the refined oxygen occupancies, those shown in Figure 4 are the most physically reasonable. All exhibit a large elongation parallel to the *c* axis (phase 1, Co−O_1/Co−O_2 = 1.21; phase 2, Co−O_1/Co−O_2 = 1.20). The 6-fold coordinate cobalt resides within a highly elongated octahedron with the five-coordinate cobalt within a similarly distorted pyramidal polyhedron. The preferred four-coordinate environment is the planar configuration shown in Figure 4. The other possible four-coordinate polyhedra provide very asymmetric environments for cobalt and have extreme bond angles. For example, a "tetrahedral" polyhedron is constrained by the O_1 oxide position to have at least one bond angle of 180°. In addition to the distorted nature of the coordination polyhedra, there is also an associated disordered twisting of the cobalt−oxygen polyhedra around the *z* axis, which moves the oxide ion at ($^1/_2$, 0, 0) to a ($^1/_2$, *y*, 0) position, where *y* is dependent on the local oxygen stoichiometry.

Attempts to refine models with ordered oxide vacancies in larger cells and lower symmetry space groups (e.g., a cell based on a slight orthorhombic distortion, $a' = \sqrt{2}a$, $b' \approx 2\sqrt{2}a$, $c' = c$ in a manner similar to that described for $Ca_2MnO_{3.5}$[3]) were unsuccessful, always resulting in the generation of the original disordered model.

The overall stoichiometry refined for this material, $LaSrCoO_{3.51(3)}$, agrees well with the value of $LaSrCoO_{3.49(1)}$ obtained by thermogravimetric reoxidation to $LaSrCoO_{4.00}$.

The small amount (0.8 mol %) of unreduced $LaSrCoO_4$ starting material observed in this sample illustrates the recurring problem of determining the correct reaction duration for the hydrogen reduction of $LaSrCoO_4$, especially with large samples. If samples are left to reduce for longer periods of time than the ideal duration, for the reduction to proceed further and thus eliminate the small quantity of starting material still observed, weak diffraction reflections due to La_2O_3 (the most

Table 1. Structural Results for the Two-Phase Refinement of Time-of-Flight Powder Neutron Diffraction Data Collected on the HRPD Instrument and Laboratory X-ray Powder Diffraction Data Collected at Room Temperature from a Sample of $LaSrCoO_{3.51(3)}$ Synthesized via the Reduction of $LaSrCoO_4$ under Flowing 8% H_2 in N_2

atom	*x*	*y*	*z*	U_{11} (Å^2)	U_{22} (Å^2)	U_{33} (Å^2)	Uiso$_{equiv}$ (Å^2)	fraction	site symmetry
Phase 1: Space Group, *I*4/*mmm*, $LaSrCoO_{3.432(8)}$									
Co	0	0	0	0.0058(5)	0.0058(5)	0.014(2)	0.0086	1	2*a* 4/*mmm*
La	0	0	0.35496(8)	0.0123(2)	0.0123(2)	0.0075(3)	0.0107	0.5	4*e* 4*mm*
Sr	0	0	0.35496(8)	0.0123(2)	0.0123(2)	0.0075(3)	0.0107	0.5	4*e* 4*mm*
O_1	0	0	0.1713(1)	0.0177(3)	0.0177(3)	0.0125(4)	0.0160	1	4*e* 4*mm*
O_2	0.5	0.045(2)	0				0.0060(3)	0.179(1)	8*j* *m*2*m*
O_3	0.5	0.135(2)	0				0.0060(3)	0.179(1)	8*j* *m*2*m*
a = 3.74544(8) Å; c = 13.3408(2) Å; V = 187.14(1) Å^3									
mole fraction: 42.5(1)%									
Phase 2: Space Group, *I*4/*mmm*, $LaSrCoO_{3.57(1)}$									
Co	0	0	0	0.0058(5)	0.0058(5)	0.014(2)	0.0086	1	2*a* 4/*mmm*
La	0	0	0.35482(7)	0.0123(2)	0.0123(2)	0.0075(3)	0.0107	0.5	4*e* 4*mm*
Sr	0	0	0.35482(7)	0.0123(2)	0.0123(2)	0.0075(3)	0.0107	0.5	4*e* 4*mm*
O_1	0	0	0.17012(9)	0.0177(3)	0.0177(3)	0.0125(4)	0.0160	1	4*e* 4*mm*
O_2	0.5	0.031(3)	0				0.0060(3)	0.197(2)	8*j* *m*2*m*
O_3	0.5	0.119(2)	0				0.0060(3)	0.197(2)	8*j* *m*2*m*
a = 3.74636(8) Å; c = 13.3201(2) Å; V = 186.95(1) Å^3									
mole fraction: 56.7(1)%									
Phase 3: Space Group, *I*4/*mmm*, $LaSrCoO_4$									
a = 3.8052(3) Å, c = 12.540(1) Å, V = 181.57(4) Å^3									
mole fraction: 0.8(1)%									
overall stoichiometry of sample: $LaSrCoO_{3.51(3)}$									

	wRp	Rp
backscattering	0.0539	0.0441
90° bank	0.0743	0.0598
X-ray	0.0624	0.0491
total	0.0592	0.0500
χ^2 = 2.441		

Table 2. Refined Parameters for Single Phase $LaSrCoO_{3.38}$ at Room Temperature from Neutron Powder Diffraction Data Collected on D2B at Two Wavelengths

atom	*x*	*y*	*z*	U_{11} (Å^2)	U_{22} (Å^2)	U_{33} (Å^2)	Uiso$_{equiv}$ (Å^2)	fraction	site symmetry
Phase 1: $LaSrCoO_{3.38(2)}$									
Co	0	0	0	0.011(1)	0.011(1)	0.023(3)	0.0159	1	2*a* 4/*mmm*
La	0	0	0.35488(7)	0.0154(4)	0.0154(4)	0.0146(7)	0.0152	0.5	4*e* 4*mm*
Sr	0	0	0.35488(7)	0.0154(4)	0.0154(4)	0.0146(7)	0.0152	0.5	4*e* 4*mm*
O_1	0	0	0.1706(1)	0.0175(6)	0.0175(6)	0.023(1)	0.0194	1	4*e* 4*mm*
O_2	0.5	0.0456(3)	0				0.0044	0.174(3)	8*j* *m*2*m*
O_3	0.5	0.1196(4)	0				0.0044	0.171(2)	8*j* *m*2*m*
a = 3.7419(1) Å; c = 13.2712(5) Å; V = 185.82(2) Å^3									

	wR_p	R_p	R_F^2
1.59 Å	0.0422	0.0331	0.0751
2.39 Å	0.0669	0.0522	0.0788
total	0.0497	0.0380	
χ^2 = 1.719			

Table 3. Refined Bond Lengths (Å) and Angles (°) for All the Refined Phases of $LaSrCoO_{3.5-x}$

		HRPD H_2		HRPD NaH			
bond	$LaSrCoO_4$	phase 1	phase 2	phase 1	phase 2	ILL 298 K	ILL 5 K
Co−O_1	2.038	2.285(2)	2.266(2)	2.257(4)	2.270(3)	2.264(1)	2.252(1)
Co−O_2	1.903	1.88802(2)	1.8777(3)	1.8783(4)	1.8784(4)	1.8787(3)	1.877(1)
Co−O_3		1.9397(4)	1.9260(6)	1.9223(4)	1.9294(4)	1.9237(3)	1.914(2)
Co−La/Sr	3.217	3.279(1)	3.279(2)	3.275(1)	3.268(1)	3.2726(6)	3.2614(7)
La/Sr−O_1	2.405	2.450(1)	2.460(1)	2.442(5)	2.451(5)	2.445(1)	2.444(2)
	2.705	2.671(2)	2.669(2)	2.6713(5)	2.6707(5)	2.6675(2)	2.6621(2)
La/Sr−O_2	2.594	2.578(3)	2.610(3)	2.601(1)	2.572(1)	2.5690(7)	2.542(8)
		2.812(2)	2.776(2)	2.774(1)	2.791(1)	2.8067(7)	2.813(9)
La/Sr−O_3		2.369(4)	2.402(4)	2.408(2)	2.376(2)	2.3947(8)	2.397(7)
		3.066(3)	3.021(2)	3.000(1)	3.025(1)	3.0141(6)	2.986(8)
Co−O_2−Co	180	169.7(3)	172.6(3)	172.4(4)	170.3(4)	169.5(2)	168.1(7)
Co−O_3−Co		149.7(6)	153.1(2)	154.3(5)	151.9(3)	153.0(2)	154.4(4)
stoichiometry	$LaSrCoO_4$	$LaSrCoO_{3.42(1)}$	$LaSrCoO_{3.52(8)}$	$LaSrCoO_{3.424(8)}$	$LaSrCoO_{3.33(1)}$	$LaSrCoO_{3.38(2)}$	$LaSrCoO_{3.39(1)}$

visible decomposition product to powder X-ray diffraction) are seen in powder X-ray diffraction patterns of the reduced material, corresponding to the decomposition of $LaSrCoO_{3.5-x}$ to La_2O_3, SrO, and Co as observed by thermogravimetric analysis (see Figure 1).

To make pure samples of $LaSrCoO_{3.5}$, NaH reductions, as described above, were performed at 200 °C employing reaction (1):

$$LaSrCoO_4 + xNaH \rightarrow LaSrCoO_{4-x} + xNaOH \quad (1)$$

Neutron powder diffraction data collected on the HRPD instrument from a sample reduced by the NaH method (sample B) were also refined in the *I*4/*mmm* space group. These data show no observable $LaSrCoO_4$ impurity, but in common with those of the sample reduced under flowing hydrogen, required the use of two reduced phases to achieve a satisfactory fit ($\chi^2 = 2.057$ for one phase; $\chi^2 = 1.321$ for two phases). The fit to the data employing a two-phase model is shown in Figure S2, with the structural data in Table S3 (Supporting Information) and refined bond lengths in Table 3. In common with the material prepared by hydrogen reduction it can be seen that the lattice parameters and bond lengths of the two phases reflect their differing local oxygen stoichiometries. The overall refined stoichiometry of $LaSrCoO_{3.36(1)}$ agrees well with the value of $LaSrCoO_{3.38(1)}$ obtained by thermogravimetric reoxidation.

The maximum *d* spacing accessible on HRPD (~3.5 Å for the 90° detector bank) could make the observation of enlarged cells, due to oxide vacancy ordering, difficult. Neutron data from an additional 5-g sample of $LaSrCoO_{3.5-x}$, reduced via the NaH technique (sample C), were collected on the D2B diffractometer at two different wavelengths (1.59 and 2.38 Å) to gain extra sensitivity, via the long wavelength data set, to any Bragg scattering at large *d* spacings. The neutron powder diffraction data indicate that, in common with the previous sample reduced via the NaH technique, there is no observable $LaSrCoO_4$ impurity present in this sample. In addition, this constant wavelength data set can be fitted adequately with a single reduced $LaSrCoO_{3.5-x}$ phase. This can be explained as a combination of the lower spatial resolution of the D2B diffractometer relative to the HRPD instrument (HRPD: $\Delta d/d = 4 \times 10^{-4}$; D2B: $\Delta d/d = 4 \times 10^{-3}$ at $2\theta = 45°$) and a smaller range of stoichiometries in the measured sample. It should be noted however that the differing spatial resolutions of the diffractometers will not have a major influence on the success, or otherwise, of a single-phase model as the resolution of the D2B diffractometer is sufficient to resolve the different *c* lattice parameters of the two phases refined for sample B ($\Delta c/c \approx 2 \times 10^{-3}$ for sample B) The addition of a second phase to the profile refinement of sample C does improve the "goodness of fit" parameters slightly ($\chi^2 = 1.719$ for one phase; $\chi^2 = 1.665$ for two phases), but its inclusion cannot be justified as the difference in lattice parameters between the two phases is of a similar magnitude to their errors (phase 1: $a = 3.736(3)$ Å, $c = 13.287(1)$ Å; phase 2: $a = 3.745(3)$ Å, $c = 13.283(1)$ Å; $\Delta a = 0.009(6)$ Å, $\Delta c = -0.004(2)$ Å) and is much smaller than the differences seen in the time-of-flight data ($\Delta a = 0.0047(1)$ Å, $\Delta c = -0.0312(5)$ Å for NaH sample).

Figure 5 shows the one-phase fit to the data sets collected at 1.59 and 2.38 Å which were refined simultaneously. The structural parameters obtained are given in Table 2 and refined bond lengths in Table 3. It can be seen from the data collected at 2.38 Å there is no evidence for the existence of a larger supercell.

Annealing experiments performed on $LaSrCoO_{3.5-x}$ samples at temperatures in the range $400 < T/°C < 600$, with the aim of equilibrating the reduced phases present and possibly ordering the oxide ion vacancies, resulted in the formation of mixtures of $LaSrCoO_{3.5-x}$ and small amounts of $LaSrCoO_4$ (~5 mol % from X-ray powder diffraction). This was presumably due to reoxidation of the reduced phases by small amounts of water or oxygen present within the sealed apparatus. Reoxidation was observed even when Li or Zr getters were present to remove any remnant oxidants, demonstrating $LaSrCoO_{3.5-x}$ to be a very powerful oxygen getter in its own right at these temperatures. However, $LaSrCoO_{3.5-x}$ is not highly air sensitive at room temperature. The reoxidative thermogravimetric data (Figure S3, Supporting Information) show that $LaSrCoO_{3.5-x}$ does not start to gain mass rapidly until over 200 °C, even under pure oxygen. This is confirmed by the fact that there is no observable change to X-ray powder diffraction patterns of samples exposed to the air for up to a week. Over longer periods of time (3−4 weeks) broad diffraction features, which can be assigned as $LaSrCoO_4$, begin to appear; however, strong diffraction reflections from the Co(II) phase can clearly be seen, even after 6 months.

Magnetic Characterization. Magnetization−field isotherms collected from a sample with a refined stoichiometry of $LaSrCoO_{3.38}$ (sample C), measured as described above, were readily fitted to linear functions. The fit to a typical isotherm is shown in Figure 6a. The fitted paramagnetic susceptibility gained from these data, shown in Figure 6b, exhibits behavior consistent with antiferromagnetic ordering ($T_N \approx 110$ K, defined as the temperature at which $\partial\chi/\partial T$ is maximum).

A plot of the reciprocal of the molar paramagnetic susceptibility against temperature fits a linear function at high temperature ($T > 160$ K), as shown in the inset to Figure 6b, suggesting Curie−Weiss behavior ($\chi = C/(T - \theta)$) in this temperature range. The value of the Curie constant extracted ($C = 3.105(9)$, corresponding to a moment of 4.98 μ_B) is significantly higher than the maximum expected moment for the system (76% high-spin Co(II) + 24% high-spin Co(I): 3.65 μ_B). However, the value of the Weiss constant extracted from the data ($\theta = -457(8)$ K) demonstrates that the Curie−Weiss law does not apply but is consistent with strong antiferromagnetic coupling of the cobalt spins.

The intercept of the linear fit to the magnetization−field isotherms, which corresponds to the saturated ferromagnetic contribution to the sample magnetization, also shows a large increase below 150 K (in addition to the value due to the Co impurity), indicating that if the material is ordering antiferromagnetically, there is significant canting of the magnetic moments leading to overall weak ferromagnetism. The ordered ferromagnetic moment is calculated to be 0.022 μ_B per cobalt ion assuming (i) the contribution from the ferromagnetic impurity remains constant in the measured temperature range and (ii) all cobalt centers contribute to the ordered ferromagnetic moment equally. (The refined stoichiometry of $LaSrCoO_{3.38(2)}$ implies 76% Co(II) and 24% Co(I).)

The neutron powder diffraction data collected at 5 K shows a series of additional Bragg reflections compared to a data set collected at 298 K from the same sample, confirming the phase is magnetically ordered. These additional Bragg reflections were assigned as being due to magnetic scattering and can be indexed with a

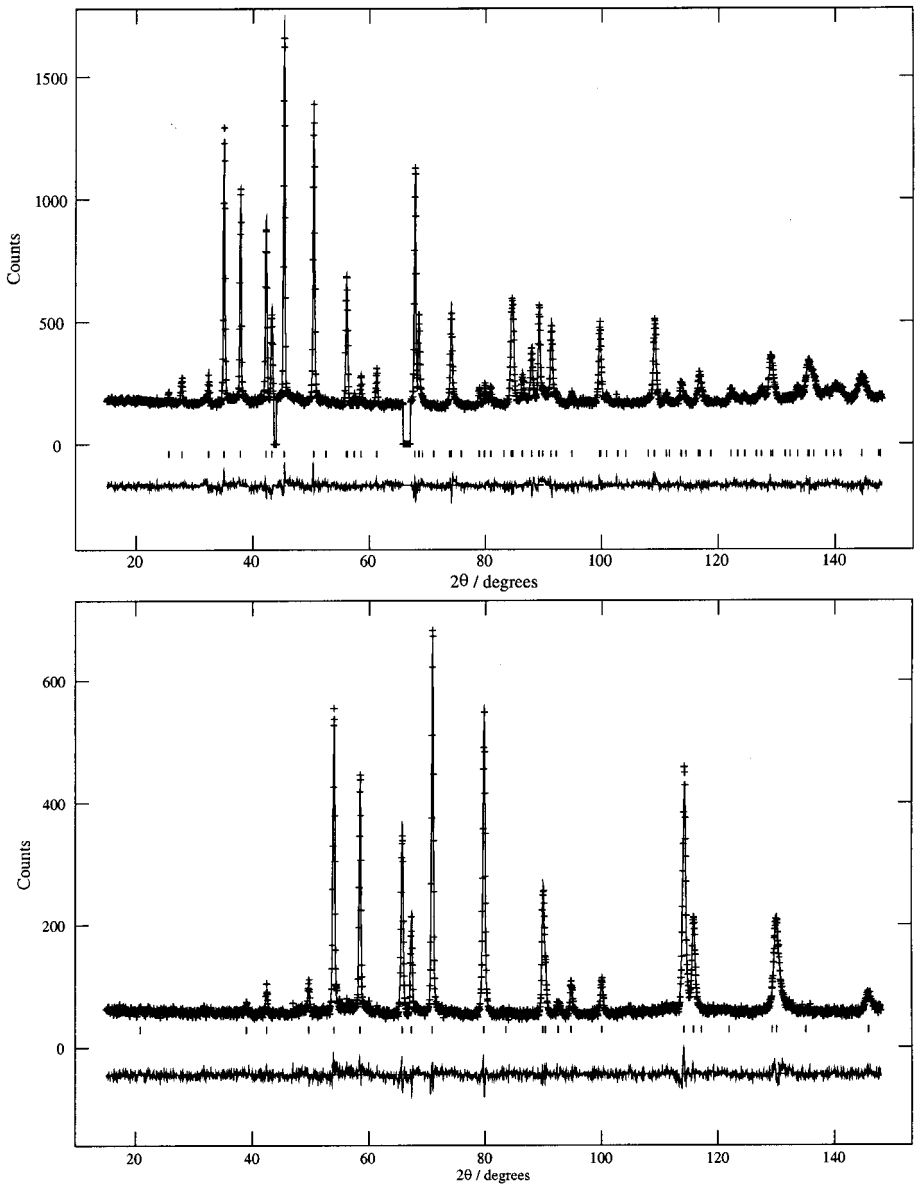

Figure 5. Observed, calculated, and difference plots for the Rietveld profile refinement of (a) 1.59 Å and (b) 2.38 Å D2B diffraction data collected from a 5-g sample of $LaSrCoO_{3.38(2)}$ reduced with NaH.

primitive tetragonal cell with lattice parameters $a_{magnetic} = \sqrt{2} \times a_{nuclear}$ and $c_{magnetic} = c_{nuclear}$.

The systematic absences observed in the magnetic Bragg peaks (no observable 00*l* reflections) suggest that the ordered moments in the system might be aligned parallel to the *z*-axis. However, none of the antiferromagnetic ordering arrangements tested with this alignment gave a satisfactory fit to the observed intensities of the magnetic reflections. It was therefore necessary to consider the existence of an ordered component of moment in the *xy* plane. Considering the observed expansion of the magnetic cell, relative to the crystallographic cell, there are two possible magnetic ordering models to describe the in-plane cobalt moments, those of La_2CuO_4 and Pr_2CuO_4.[11] Both consist of alternate sheets of ferromagnetically aligned spins, as shown in Figure 7a, with the magnetic spin vectors being perpendicular to the plane of the ferromagnetic sheet in the Pr_2CuO_4 model and parallel in the La_2CuO_4 model. The presence of a strong 100 magnetic reflection would appear to indicate that the former model is the more appropriate one for $LaSrCoO_{3.5-x}$ as the alignment of the moments perpendicular to the ferromagnetic sheets (and therefore the translational symmetry vectors) in the Pr_2CuO_4 model leads to the 100 magnetic reflection being systematically absent, although it should be noted that any component of the spin vector parallel to the *z*-axis would produce intensity in the 100 reflections, regardless of which ordering model is adopted. Rietveld profile refinement of the low-temperature neutron powder diffraction data employing the nuclear model refined at 298 K and the La_2CuO_4 magnetic ordering model with the addition of a component of the ordered magnetic moment parallel to the *z* axis provided a good fit to the low-temperature neutron powder diffraction data and yielded a collinear antiferromagnetically ordered model as shown in Figure 7a.

It can be seen that this model has orthorhombic symmetry. However, there is no evidence in the low-

(11) Cox, D. E.; Goldman, A. I.; Subramanian, M. A.; Gopalakrishnan, J.; Sleight, A. W. *Phys. Rev. B* **1989**, *40*, 6998.

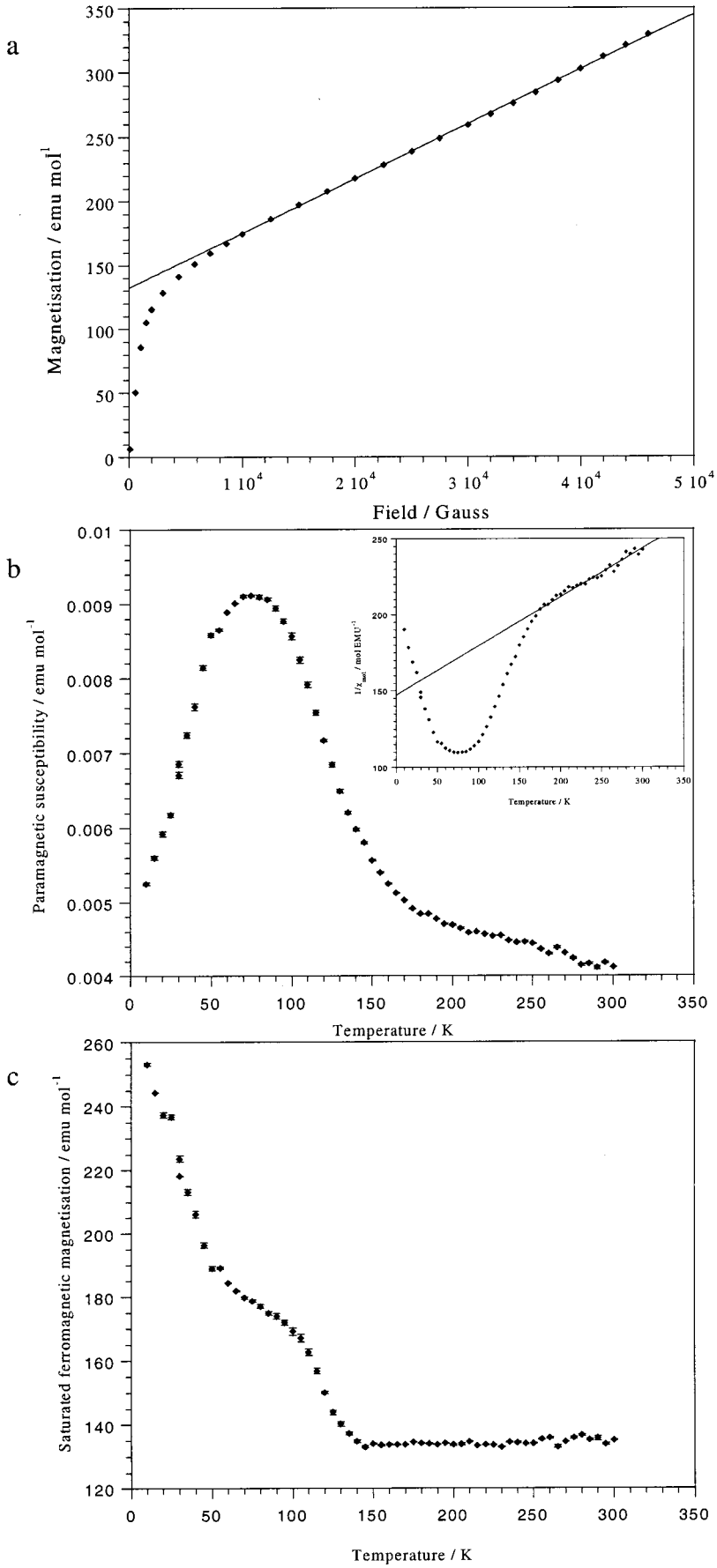

Figure 6. (a) Typical linear fit to a magnetization−field isotherm of $LaSrCoO_{3.38(2)}$ at 300 K showing the linear region in applied fields greater than 20 kG. (b) Fitted paramagnetic susceptibility plotted against temperature. Inset shows the linear fit to $1/\chi_{mol}$ at high temperature ($T > 150$ K). The values of C and θ obtained from the Curie−Weiss law ($\chi = C/(T - \theta)$) are $C = 3.105(9)$, $\theta = -457(8)$ K. (c) Saturated ferromagnetic magnetization plotted against temperature for a sample $LaSrCoO_{3.38(2)}$ synthesized via the reduction of $LaSrCoO_4$ with NaH.

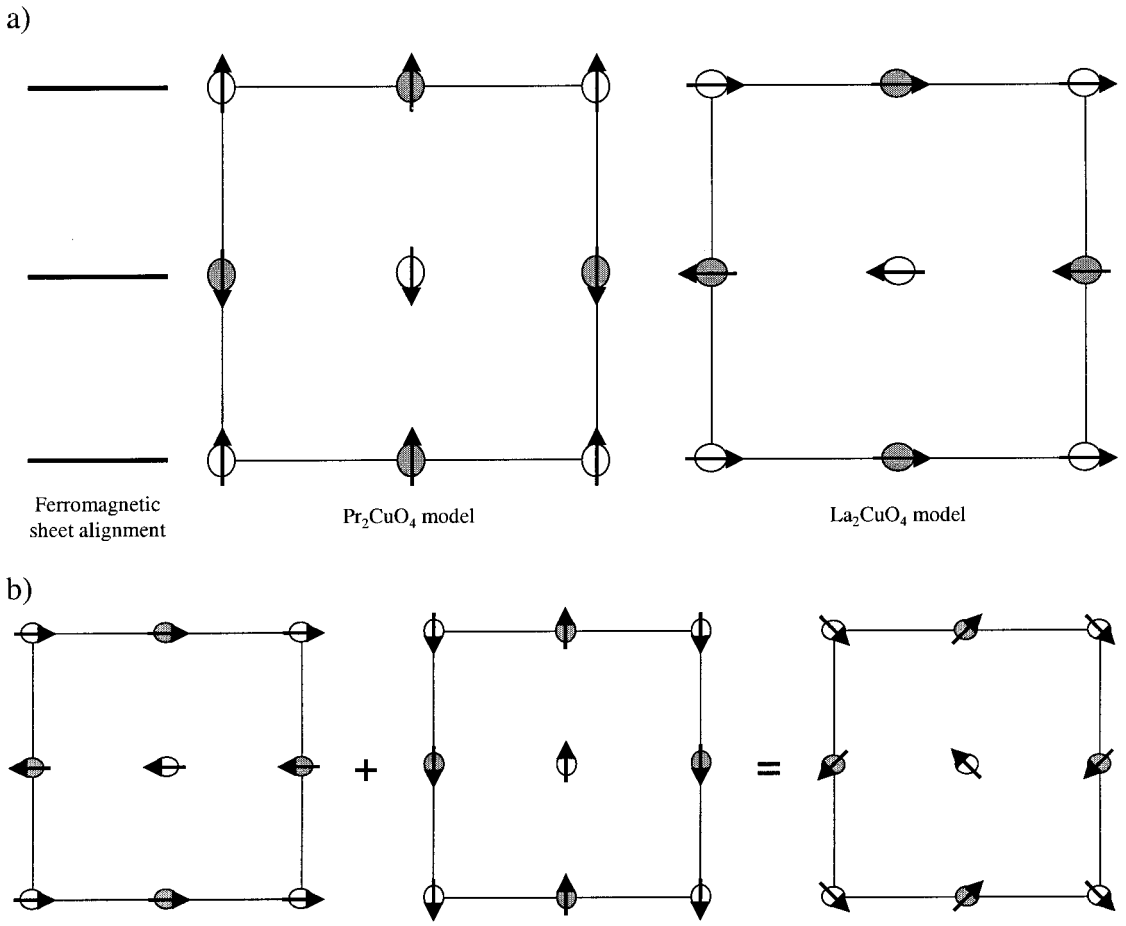

Figure 7. (a) Possible ordering models for the in-plane components of the magnetic vectors of $LaSrCoO_{3.38(2)}$ viewed along [001]. Open atoms are at $z = 0$; shaded atoms are at $z = {}^1/_2$. (b) Relation between the collinear orthorhombic and noncollinear tetragonal descriptions of the ordered moments of $LaSrCoO_{3.38(2)}$. Open atoms are at $z = 0$; shaded atoms are at $z = {}^1/_2$.

temperature diffraction data to suggest a splitting or broadening of diffraction reflections which would occur on a lowering of the cell symmetry from tetragonal to orthorhombic. Therefore, a noncollinear description of the magnetic ordering is favored. A tetragonal noncollinear ordering model can be constructed by the addition of the collinear model to a counterpart formed by 90° rotation about *z*, as described for the case of Pr_2CuO_4 by Cox et al.,[11] to yield an ordering regime as shown in Figure 7b. The fit to the low-temperature data employing both nuclear and magnetic scattering models is shown in Figure 8a with the three-dimensional ordering of the magnetic moments described in Figure 8b and Table 4 and refined bond lengths in Table 3. The weak ferromagnetic moment observed in the magnetization data is too small to be observable in the low-temperature diffraction pattern and so is not included in the model for the magnetic structure.

Discussion

Reduction of $LaSrCoO_4$ to $LaSrCoO_{3.5-x}$ can be readily effected by employing flowing 8% H_2 in N_2 or NaH as reducing agents. The reduction is topotactic and introduces oxide ion vacancies into the $Co-O_{equatorial}$ planes with no observable long-range translational order. Examination of the structural data refined for the single-phase sample (sample C) shows the reduction is accompanied by reduction in the *a* lattice parameter ($a_{reduced} = 3.745$ Å, $a_{unreduced} = 3.810$ Å). However, the in-plane cobalt oxygen bond distances are not reduced significantly with this lattice contraction due to the twisting of the cobalt−oxygen polyhedra ($Co-O_2$ $LaSrCoO_4$, 1.903 Å; average in-plane Co−O $LaSrCoO_{3.38}$, 1.901 Å). The contraction of *a* can be seen to be driven by the coordination requirements of the La/Sr ions (Figure 4c). Upon reduction the A cation site is reduced from being nine-coordinate to a mixture of 8- and 7-coordination (depending on the local cobalt oxidation state), necessitating the observed contraction of the local coordination sphere, which is most easily achieved in the *xy* plane ($La/Sr-O_1$ bond lengths $4 \times 2.6675(2)$ Å in $LaSrCoO_{3.38}$ compared with 4×2.705 Å in $LaSrCoO_4$). This contraction forces the Co−O polyhedra to twist around an axis parallel to *z*, to maintain the $Co-O_{equatorial}$ bond lengths and demonstrates the reduction in rigidity of the structure on the introduction of oxide vacancies. The crystallographic splitting of the equatorial oxide position (O_2 and O_3) is an indication that despite an acceptable fit to a single-phase model there is still a significant degree of inhomogeneity in the oxygen stoichiometry of this sample. In addition to the reduction in the *a* lattice parameter, there is a dramatic increase in the *c* parameter. The origin of this increase can be seen to be due to a cooperative distortion of the cobalt oxygen polyhedra ($LaSrCoO_{3.39}$:$Co-O_{axial}/Co-O_{equatorial} = 1.1908(7)$, $LaSrCoO_4$:$Co-O_{axial}/Co-O_{equatorial} = 1.070$[9]), analogous to that observed in $La_2Co_2O_5$ where

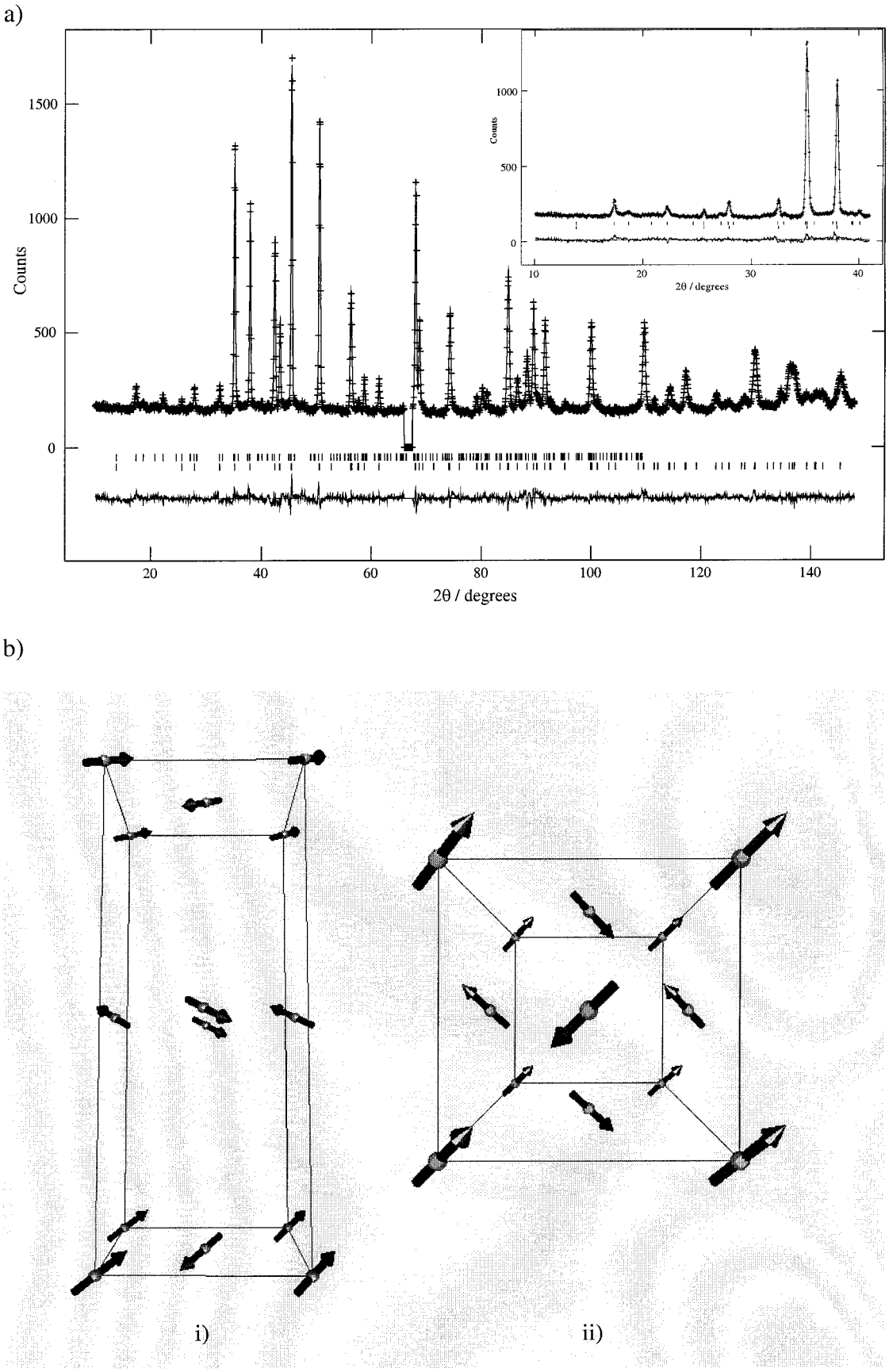

Figure 8. (a) Observed, calculated, and difference plots for the Rietveld profile refinement of 5 K neutron powder diffraction data collected from a 5-g sample of $LaSrCoO_{3.38(2)}$ reduced with NaH, employing both nuclear (lower tick marks) and magnetic (upper tick marks) models. (b) Three-dimensional projection of the refined magnetic structure of $LaSrCoO_{3.38(2)}$ viewed (i) along the [010] axis and (ii) along the [001] axis.

Table 4. Structural and Magnetic Results for Refinement of Powder Neutron Diffraction Data Collected at 5 K from a Sample of $LaSrCoO_{3.38(2)}$ Synthesized via the Reduction of $LaSrCoO_4$ with NaH (3 × 4 days, 200 °C)

atom	*x*	*y*	*z*	U_{11} (Å^2)	U_{22} (Å^2)	U_{33} (Å^2)	$U\text{iso}_{\text{equiv}}$ (Å^2)	fraction	site symmetry
Phase 1: Space Group, *I*4/*mmm*, $LaSrCoO_{3.39(1)}$									
Co	0	0	0	0.012(1)	0.012(1)	0.009(2)	0.0113	1	2*a* 4/*mmm*
La	0	0	0.35523(8)	0.0100(3)	0.0100(3)	0.0153(7)	0.0118	0.5	4*e* 4*mm*
Sr	0	0	0.35523(8)	0.0100(3)	0.0100(3)	0.0153(7)	0.0118	0.5	4*e* 4*mm*
O_1	0	0	0.1703(1)	0.0106(5)	0.0106(5)	0.024(1)	0.0151	1	4*e* 4*mm*
O_2	0.5	0.052(3)	0				0.0037(7)	0.173(3)	8*j* *m*2*m*
O_3	0.5	0.112(3)	0				0.0037(7)	0.172(3)	8*j* *m*2*m*
a = 3.73439(5) Å; c =13.2220(2) Å; V = 184.390(5) Å^3									

atom	*x*	*y*	*z*	M_x/μ_B	M_y/μ_B	M_z/μ_B	$\lvert M\rvert/\mu_B$
Co	0	0	0	0.87(3)	0.87(3)	0.54(7)	1.35(3)
Co	0.5	0.5	0	−0.87(3)	−0.87(3)	−0.54(7)	1.35(3)
Co	0.5	0	0.5	0.87(3)	−0.87(3)	−0.54(7)	1.35(3)
Co	0	0.5	0.5	−0.87(3)	0.87(3)	0.54(7)	1.35(3)

	wRp	Rp
1.59 Å	0.0463	0.0366
	χ^2 = 2.202	

$Co-O_{axial}/Co-O_{equatorial}$ = 1.17(2), 1.12(1) for the octahedrally coordinated cobalt.[7] The cobalt−oxygen coordination polyhedra observed in $LaSrCoO_{3.38}$ (sample C) are highly unusual (Figure 4b), suggesting that what we observe is in fact the product of averaging over different ordered microdomains. This averaging occurs only within the CoO_{2-x} layers as the $Co-O_1$ bonds are well defined; their lengths show that the CoO_x (x = 4, 5, 6) polyhedra within the domains must be strongly elongated along the stacking direction. The phase separation observed (samples A and B) is also consistent with such local ordering. The material is able to support long-range magnetic order, demonstrating that the long-range disordering of the anions does not disrupt the short-range superexchange interactions, again consistent with local microdomain formation.

Thermogravimetric analysis of materials synthesized by the reduction of $LaSrCoO_4$, with hydrogen gas or NaH, show that the samples produced can adopt compositions within a narrow range of oxygen stoichiometry. Furthermore, the need to use multiphase models to adequately fit the high-resolution powder neutron diffraction data indicates that under these reducing conditions phases within this small stoichiometry range can coexist. The bond lengths of the cobalt oxygen coordination polyhedra, in these phases, are very sensitive to the oxidation state of cobalt. Therefore, a comparison of these parameters between the phases simultaneously refined for a particular sample provides some measure of the inhomogeneity in the oxygen stoichiometry present within that sample. Such a comparison shows that, of the two materials measured on HRPD (samples A and B), the cobalt−oxygen polyhedra in the two phases refined for the material reduced by NaH are less different than those refined for the material reduced by hydrogen gas ($\Delta Co-O_1$: 0.019(5) Å (H_2), 0.013(7) Å (NaH); $\Delta Co-O_2$: 0.0025(5) Å (H_2), 0.0001(8) Å (NaH); $\Delta Co-O_3$: 0.0137(10) Å (H_2), 0.0071(8) Å (NaH)), indicating a lower level of inhomogeneity in the oxygen stoichiometry of the NaH reduced material. This agrees with the experimental observation of $LaSrCoO_4$ present in the hydrogen-reduced sample. The need to employ only one phase to model the sample measured on D2B indicates this sample has an even lower level of inhomogeneity in the oxygen stoichiometry and shows a small difference in reaction conditions (sample B: 2 × 5 days, 200 °C; sample C: 3 × 4 days 200 °C) has a large effect on homogeneity of the sample produced. We can therefore conclude that NaH allows access to lower cobalt oxidation states than H_2 and yields more homogeneous products.

The absence of a well-defined product stoichiometry could be explained by the observation that the oxide ion vacancies exhibit no long-range order over the length scales that can be detected by X-ray or neutron diffraction. This disordering of the vacancies within the *xy* plane allows a degree of structural flexibility which in turn will relax the stringent stoichiometric requirements imposed by a highly ordered three-dimensional structure, leaving the number of oxide ion vacancies to be largely defined by the oxidation state preferences of cobalt. An alternative possibility is the presence of ordered microdomains within the material, with dimensions too small to be observed by bulk diffraction, which allow a degree of stoichiometric flexibility. The refined structures would then be an average over the true structure in each microdomain. Detailed HRTEM imaging and diffraction studies are required to resolve this issue.

Long-range translational ordering of the anion locations, observed in $Ca_2MnO_{3.5}$,[3] does not occur for $LaSrCoO_{3.5-x}$. This retention of tetragonal symmetry upon reduction is also found for $NdSrCuO_{3.56}$, in which the oxide anion vacancies are distributed between both the axial (occupancy = 0.92) and equatorial (occupancy = 0.86) sites.[12] In the present case, the anion vacancies are confined to the MO_2 planes and thus the orthorhombic distortion found for $La_{1.6}Sr_{0.4}NiO_{3.47}$ due to differential occupancy of the (0, $^1/_2$, 0) and ($^1/_2$, 0, 0) positions might be expected.[13] Hence, the combination of the disordering of the anion vacancies within the CoO_{2-x} layer to retain tetragonal translational symmetry and the rotation of the resulting CoO_5 units about the $Co-O_{axial}$ bonds is novel.

(12) Labbe, P. H.; Ledesert, M.; Caignaert, V.; Raveau, B. *J. Solid State Chem.* **1991**, *91*, 362.
(13) Crespin, M.; Basat, J. M.; Odier, P.; Mouron, P.; Choisnet, J. *J. Solid State Chem.* **1990**, *84*, 165.

The observation of a small ferromagnetic impurity in the magnetization data of all the $LaSrCoO_{3.5-x}$ samples can be readily assigned as being due to impurities of metallic cobalt at the 0.5−1.5 mol % level (T_c = 1395 K). Using the procedure outlined above, this impurity signal can be removed to reveal the high-field magnetic behavior of the bulk material. The magnetization data show that $LaSrCoO_{3.5-x}$ orders antiferromagnetically at $T_N \approx 110$ K. Above 150 K the reciprocal of the paramagnetic susceptibility is linear with temperature but the large Weiss constant ($\theta = -457(8)$ K) indicates the Curie−Weiss law does not apply due to strong antiferromagnetic coupling between the cobalt spins. This can be interpreted as being due to two-dimensional antiferromagnetic coupling of cobalt spins within but not between the transition metal MO_{2-x} layers, with three-dimensional ordering not occurring until 110 K. This is supported by the high Néel transition temperatures observed in the materials synthesized via reduction of three-dimensional perovskite phases ($La_2Co_2O_5$: T_N = 310 K[7]).

The saturated ferromagnetic moment of the sample (measured as the intercept at the zero field of the linear fit to the magnetization−field isotherms) shows a sharp rise coincident with the onset of antiferromagnetic ordering, observed in the paramagnetic susceptibility (Figure 6). This is interpreted as canting of the ordered antiferromagnetic moments relative to each other, resulting in weak ferromagnetism. The resultant ordered ferromagnetic moment is calculated to be 0.022 μ_B per cobalt ion.

Neutron powder diffraction data collected at 5 K confirm the presence of antiferromagnetic order within the material, validating the procedure used to determine the magnetic susceptibility, and allows the refinement of a noncollinear antiferromagnetic ordered model with tetragonal symmetry consistent with the observed crystallographic symmetry.

The determination of the spin states of the cobalt centers within the $LaSrCoO_{3.5-x}$ system is complicated by the mixed cobalt valence exhibited. The large moment extracted from the susceptibility data would appear to suggest a high-spin configuration for both Co(II) and Co(I) centers. However, the large Weiss constant associated with this moment makes it unreliable. In addition, the possibility that small particles of elemental cobalt within the sample are behaving superparamagnetically, rather than ferromagnetically, means this extracted value for the moment should be considered an upper limit.

Studies by Hansteen et. al. of the reduced cobaltates $La_4Co_3O_9$[14] and two phases $La_3Co_3O_8$ and $La_2Co_2O_5$,[6,7] isolated by the reduction of $LaCoO_3$, have shown significant lattice expansions upon the reduction of low-spin Co(III) to high-spin Co(II) ($\Delta V = 5.49$ Å^3 per cobalt ion for the transition from $LaCoO_3$ to $La_2Co_2O_5$; ΔV = 4.68 Å^3 per cobalt ion for the transition from $La_4Co_3O_{10}$ to $La_4Co_3O_9$). The relatively small expansion observed upon reduction to $LaSrCoO_{3.38(2)}$ ($\Delta V = 2.39$ Å^3) would suggest the smaller low-spin configuration is adopted in this material (ionic radius of Co(II): $S = {}^1/_2$, 0.65 Å; $S = {}^3/_2$, 0.745 Å[15]). However, direct comparison of the volume changes of these different systems should only be made in light of the complicated spin state equilibria adopted by the oxidized materials.[9,16,17] Further characterization of the Co(II) spin state using refined bond lengths is complicated by the observed structural disorder within the material. One striking structural feature unaffected by the disorder is the large elongation of the cobalt−oxygen polyhedra along the *z* axis. This could be interpreted as a cooperative Jahn−Teller distortion, the magnitude of which would suggest a low-spin d^7 configuration for Co(II). However, this interpretation is not borne out in the structural data reported for other reduced Co(II) oxides which have been shown unambiguously to be in the high-spin configuration yet exhibit significant distortions in their cobalt−oxygen polyhedra.[7,14]

The ordered moment refined from the antiferromagnetically ordered structure of $LaSrCoO_{3.38(2)}$ is 1.35(3) μ_B. This value is too large to be due to the 76% Co(II) centers in a low-spin ($S = {}^1/_2$) configuration; however, it is close to the value expected for a combination of low-spin Co(II) and high-spin Co(I) (1.26 μ_B). The spin states at the cobalt centers are therefore at present unclear.

Conclusion

Reduction of $LaSrCoO_4$ can be readily be achieved, using standard gaseous hydrogen or solid sodium hydride as reducing agents, to form phases of stoichiometry $LaSrCoO_{3.5-x}$. Reduction involves the topotactic deintercalation of oxide ions from the CoO_2 planes of the (La/SrO)−(La/SrO)−(CoO_2)−(La/SrO)−(La/SrO)−(CoO_2) stacking sequence to yield a structure with oxide ion vacancies disordered throughout this plane. This regime of two dimensionally disordered vacancies, on the X-ray/neutron diffraction length scale, is unlike the three-dimensional ordering of vacancies seen in the materials synthesized via the reduction of the related perovskite phase, $LaCoO_3$. Magnetic long-range order is observed in $LaSrCoO_{3.5-x}$, however, despite the absence of long-range vacancy ordering.

In addition to the positional disorder of the oxide ion vacancies, the drive for the La/Sr cation site to contract its local coordination shell to adjust to a lower coordination number upon reduction and the need to accommodate the longer Co(II)−O bond lengths lead to a twisting of cobalt−oxygen polyhedra around the *z* axis. A comparison of the reduced material synthesized via the different reduction techniques shows that sodium hydride allows access to lower mean oxidation states than flowing hydrogen (refined stoichiometries: H_2, $LaSrCoO_{3.51(3)}$; NaH, $LaSrCoO_{3.38(2)}$) and in addition the products of hydride reduction have lower levels of inhomogeneity in their oxygen stoichiometry.

Reduction of $LaSrCoO_4$ to materials of stoichiometry $LaSrCoO_{3.5-x}$ implies Co(I) ions are present. This is highly unusual in an extended oxide and illustrates the reducing power of NaH under the conditions of the reaction. A number of Co(I) oxides have been prepared

(14) Hansteen, O. H.; Fjellvag, H.; Hauback, B. C. *J. Mater. Chem.* **1998**, *8*, 2089.

(15) Shannon, R. D.; Prewitt, C. T. *Acta Crystallogr.* **1970**, *B26*, 1046.

(16) Hansteen, O. H.; Fjellvag, H. *J. Solid State Chem.* **1998**, *141*, 212.

(17) Senaris-Rodriguez, M. A.; Goodenough, J. B. *J. Solid State Chem.* **1994**, *116*, 224.

(CsK_2CoO_2[18], K_3CoO_2[19]), but they are very different from the $LaSrCoO_{3.5-x}$ phases described here, consisting of isolated CoO_2^{3-} anion units rather than the extended coordination structure observed for the $LaSrCoO_{3.5-x}$ phases.

The high concentration of Co(I) in the $LaSrCoO_{3.5-x}$ materials (24 mol % in $LaSrCoO_{3.38}$) would suggest that it may be possible to reduce the cobalt oxidation state even further and prepare an extended Co(I) oxide phase by topotactic reduction with metal hydrides. The scope of metal hydride reagents for the synthesis of vacancy-ordered metal oxides with the cations in novel oxidation states has yet to be fully defined.

(18) Bernhardt, F.; Hoppe, R.; Kremer, R. K. *Z. Anorg. Allg. Chem.* **1994**, *620*, 187.
(19) Burow, W.; Birx, J.; Bernhardt, F.; Hoppe, R. *Z. Anorg. Allg. Chem.* **1993**, *619*, 923.

Acknowledgment. We thank Dr T. Hansen for his expert assistance with the collection of powder neutron diffraction data at the Institut Laue Langevin, Grenoble. M.A.H. thanks the EPSRC for a studentship.

Supporting Information Available: Rietveld profile refinement of HRPD backscattering data from $LaSrCoO_{3.51(3)}$; observed, calculated, and difference plots for the Rietveld profile refinement of a (a) HRPD backscattering bank, (b) HRPD 90° bank, and (c) powder X-ray diffraction data from $LaSrCoO_{3.36(2)}$; structural results for the refinement of powder neutron diffraction data collected on the D2B instrument from $LaSrCoO_{3.38(2)}$; thermogravimetric reoxidation plot for $LaSrCoO_{3.49(1)}$ under flowing O_2. This material is available free of charge via the Internet at http://pubs.acs.org.

CM9906811